

Oxidative stress by layered double hydroxide nanoparticles via an SFK-JNK and p38-NF- κ B signaling pathway mediates induction of interleukin-6 and interleukin-8 in human lung epithelial cells

Soo-Jin Choi
Hee-Jeong Paek
Jin Yu

Department of Food Science and
Technology, Seoul Women's University,
Seoul, Republic of Korea

Abstract: Anionic nanoclays are layered double hydroxide nanoparticles (LDH-NPs) that have been shown to exhibit toxicity by inducing reactive oxidative species and a proinflammatory mediator in human lung epithelial A549 cells. However, the molecular mechanism responsible for this LDH-NP-induced toxicity and the relationship between oxidative stress and inflammatory events remains unclear. In this study, we focused on intracellular signaling pathways and transcription factors induced in response to oxidative stress caused by exposure to LDH-NPs in A549 cells. Mitogen-activated protein kinase (MAPK) cascades, such as extracellular signal-regulated kinase, c-Jun-N-terminal kinase (JNK), and p38, were investigated as potential signaling mechanisms responsible for regulation of oxidative stress and cytokine release. Src family kinases (SFJs), which are known to mediate activation of MAPK, together with redox-sensitive transcription factors, including nuclear factor kappa B and nuclear factor-erythroid 2-related factor-2, were also investigated as downstream events of MAPK signaling. The results obtained suggest that LDH-NP exposure causes oxidative stress, leading to expression of antioxidant enzymes, such as catalase, glucose reductase, superoxide dismutase, and heme oxygenase-1, via a SFK-JNK and p38-nuclear factor kappa B signaling pathway. Further, activation of this signaling was also found to regulate release of inflammatory cytokines, including interleukin-6 and interleukin-8, demonstrating the inflammatory potential of LDH-NP.

Keywords: layered double hydroxide, mitogen-activated protein kinases, Src family kinases, nuclear factor kappa B, oxidative stress, inflammatory cytokine

Introduction

Nanotechnology and engineered nanoparticles have been extensively applied in diverse industrial fields, including manufacturing, processing, materials, and consumer products.^{1,2} Although nanomaterials provide many benefits related to their small size, large surface area, and high reactivity, there is growing concern about their possible adverse effects on human health.^{3,4} Further, the toxic effects of nanoparticles may be closely associated with their size-related properties.^{5,6} Of the various types of nanoparticles, inorganic layered double hydroxide nanoparticles (LDH-NPs), also known as anionic nanoclays, have attracted much attention as heat retention additives in plastic films, flame retardants, stabilizing agents for polymers, precursors of catalytic and magnetic materials, and drug delivery carriers in biology and medicine.^{7,8} LDH-NPs have the potential for widespread use due to their lamellar structures, which allow intercalation of anionic molecules between layers, enabling their controlled release and protecting them from surrounding environmental conditions.⁹

Correspondence: Soo-Jin Choi
Seoul Women's University, 621
Hwarang-ro, Nowon-gu, Seoul 139-774,
Republic of Korea
Tel +82 2 9705 634
Fax +82 2 9705 977
Email sjchoi@swu.ac.kr

The toxicity of LDH-NPs has been reported to differ according to the chemical compositions, cell lines, and concentrations used.¹⁰ Although LDH-NPs are known to be less toxic than other inorganic nanoparticles, it has been reported that they might generate reactive oxygen species (ROS) and interleukin (IL)-8, a proinflammatory mediator, in cultured cells, suggesting that LDH-NPs are potentially toxic in terms of inducing oxidative stress and inflammation.¹¹ Nanoparticle-induced oxidative stress has been reported to mediate adverse physiological responses, such as inflammation, genotoxicity, fibrosis, and carcinogenesis.¹² It has also been demonstrated that generation of ROS and inflammation have an interdependent relationship in cells exposed to nanoparticles, as a reflection of protective attempts by the cell to destroy nanoparticles.¹³ Indeed, nanoparticle-mediated oxidative stress can contribute to activation of signaling pathways involved in proinflammatory cascades.¹⁴ However, little is known about LDH-NP-induced toxicity or its molecular mechanism, and information on this would be useful for prediction of potential toxicity after prolonged exposure.

To understand the mechanism responsible for the toxicity of LDH-NPs, we evaluated the involvement of oxidative stress-responding and inflammation-regulating signal transduction pathways and of associated transcription factors. Mitogen-activated protein kinase (MAPK) cascades, such as extracellular signal-regulated kinase (ERK), c-Jun-N-terminal kinase (JNK), and p38, have been investigated as upstream signaling mechanisms responsible for regulating oxidative stress and cytokine release.^{15,16} The MAPK cascades are multifunctional signaling pathways that are initiated in response to diverse extracellular stimuli, including growth factors, oxidants, DNA damage, cytokines, toxins, and physical stress, and regulate a variety of cellular responses, such as apoptosis, induction of phase II detoxifying enzymes, immune activation, and inflammation.^{17,18} On the other hand, Src family kinases (SFKs), which are non-receptor protein tyrosine kinases, are known to mediate activation of MAPK in response to extracellular stimuli (eg, ROS or ultraviolet radiation).^{19,20} Hence, we considered that activation of SFKs could play a role in nanoparticle-induced oxidative stress and inflammation.

Redox-sensitive transcription factors implicated in LDH-NP-induced toxicity were also investigated, with a focus on nuclear factor kappa B (NF- κ B) and nuclear factor-erythroid 2-related factor-2 (Nrf-2) as downstream events in the MAPK pathway. The NF- κ B complex controls DNA transcription and is activated by harmful cellular stimuli, including oxidative stress, and consequently induces expression of a variety of proteins required for immunological and cellular defense.^{21,22}

Nrf-2 is a basic transcription factor and regulates cellular antioxidant and anti-inflammatory responses.²³ Nrf-2 dissociates from Kelch-like ECH-associated protein 1 in cytoplasm and then translocates to the nucleus, where it binds antioxidant response elements required for the transcriptional activation of genes, including cytoprotective and antioxidant genes.^{24,25} Many researchers have suggested that cytosolic NF- κ B and Nrf-2 are phosphorylated and translocated into the nucleus in response to the MAPK pathway under conditions of oxidative stress.^{26,27}

Accordingly, the aim of this study was to investigate the phenomenon of LDH-NP-induced toxicity and to determine the molecular mechanism involved by focusing on oxidative stress and inflammation, in order to better understand and predict the potential adverse effects of LDH-NPs on human health. In our previous study, because LDH-NP generated the most ROS and induced the proinflammatory mediator IL-8 in A549 human alveolar epithelial cancer cells, we used the same cell line for the present study.¹¹ Oxidative stress induced by LDH-NPs was evaluated by estimating intracellular ROS generation and antioxidant enzyme activity, including those of superoxide dismutase (SOD), catalase (CAT), and glutathione reductase (GR), in A549 lung epithelial cells. Expression of heme oxygenase-1 (HO-1), an antioxidant enzyme induced in response to oxidative stress, was also investigated. In addition, we evaluated the induction of proinflammatory cytokines, such as IL-1, IL-6, IL-8, and tumor necrosis factor α (TNF- α), in LDH-NP-treated cells. Finally, signaling pathways and transcription factors activated by LDH-NP exposure were investigated, with a focus on the relationship between oxidative stress and induction of inflammation.

Materials and methods

Preparation of nanoparticles

LDH-NPs ($\text{Mg}_{0.68}\text{Al}_{0.32}(\text{OH})_2(\text{CO}_3)_{0.16} \cdot 0.1\text{H}_2\text{O}$; particle size ~ 100 nm) were prepared by coprecipitation as described previously.¹¹ Briefly, an aqueous solution of 0.5 M NaOH/0.5 M NaHCO_3 was added dropwise to a mixed Mg/Al nitrate solution at room temperature to pH ~ 9.5 . The resulting white precipitate was kept at 100°C for 24 hours under hydrothermal conditions to obtain uniformly sized homogeneous nanoparticles. The nanoparticles were analyzed by powder X-ray diffraction (PW3710 diffractometer [Phillips, Eindhoven, the Netherlands] with Ni-filtered $\text{CuK}\alpha$ radiation [$\lambda = 1.5418$ Å]), Fourier transform infrared spectroscopy (Spectrum One B, PerkinElmer, Wellesley, MA, USA), and scanning electron microscopy (S-4300, Hitachi Tokyo, Japan). The mean particle size of the LDH-NPs was determined by randomly

selecting 200 particles in scanning electron microscopy images.

Cell culture

Human lung alveolar carcinoma epithelial (A549) cells were purchased from the Korean Cell Line Bank and cultured in Roswell Park Memorial Institute 1640 medium under a humidified atmosphere (5% CO₂/95% air) at 37°C. The medium was supplemented with 10% heat inactivated fetal bovine serum (Welgene Biopharmaceuticals, Daegu, Korea), 100 units/mL penicillin, and 100 µg/mL streptomycin.

Cell proliferation

The effect of LDH-NPs on cell proliferation was measured using the WST-1 assay (Roche, Basel, Switzerland). Briefly, cells (5×10³/100 µL) were exposed to 1–1,000 µg/mL LDH-NPs for 24 hours or 500 µg/mL LDH-NPs for times ranging from 1 hour to 24 hours. Next, 10 µL of WST-1 solution (Roche) was added to each well, and cells were incubated for a further 4 hours. Absorbance was then measured using a plate reader at 440 nm (Dynex Technologies, Chantilly, VA, USA). Cells incubated in the absence of LDH-NPs were used as the control.

Intracellular ROS generation

Intracellular ROS levels were monitored using a peroxide-sensitive fluorescent probe, carboxy-2',7'-dichlorofluorescein diacetate (H₂DCFDA, Molecular Probes, Eugene, OR, USA), according to the manufacturer's guidelines. Briefly, cells (5×10³) were incubated with the nanoparticles under standard conditions as described above, washed with phosphate-buffered saline, collected by centrifugation, and incubated with 40 µM carboxy-H₂DCFDA for 60 minutes at 37°C. After washing with phosphate-buffered saline, dichlorofluorescein fluorescence was immediately measured using a fluorescence microplate reader (SpectraMax[®] M3, Molecular Devices, Silicon Valley, CA, USA), and excitation and emission wavelengths were 490 nm and 530 nm, respectively. Cells not treated with nanoparticles were used as the control.

Antioxidant enzyme activity

The activity of CAT, GR, and SOD was estimated using a Chemical SOD assay kit (Cayman Chemical Company, Ann Arbor, MI, USA), the CAT assay kit (Enzo Life Science, Farmingdale, NY, USA), and the Chemical GR assay kit (Cayman), respectively, according to the manufacturer's protocols. Enzyme activity is presented as a percentage of the enzyme activity of controls.

Western blot analysis

Cells were exposed to nanoparticles (500 µg/mL) for designated times (1, 3, 6, 10, and 24 hours), washed twice in ice-cold phosphate-buffered saline, and harvested using a scraper. Cell pellets were then collected by centrifugation. After washing the pellets twice with phosphate-buffered saline, cell lysis RIPA buffer (Sigma-Aldrich, St Louis, MO, USA) containing protease inhibitor cocktails (Thermo Fisher Scientific Inc, Pittsburgh, PA, USA) was added, and the pellets were incubated for 20 minutes at 4°C and centrifuged at 14,000× *g* for 30 minutes at 4°C to obtain total cell lysates. Nuclear and cytosol fractions were obtained using a Nuclear/Cytosol fractionation kit (BioVision Inc, Milpitas, CA, USA) according to the manufacturer's protocol. Protein concentrations in cell lysates were determined using the Bradford assay (Bio-Rad Hercules, CA, USA).

Aliquots of lysates containing 30 µg of proteins were subjected to 10% sodium dodecyl sulfate polyacrylamide gel electrophoresis, and after transfer to polyvinylidene fluoride membranes (Millipore, Billerica, MA, USA), the blots were preblocked with 5% skim milk in Tris buffered saline-Tween 20 (TBS-T) solution (20 mM Tris-HCl, 150 mM NaCl, pH 7.4, and 0.05% Tween 20) for 4 hours, and incubated overnight with rabbit polyclonal antibodies against HO-1 (1:100, Santa Cruz Biotechnology Inc, Santa Cruz, CA, USA), p38 (1:1,000, Enzo Life Sciences), p-p38 (1:1,000), ERK (1:1,000), p-ERK (1:200), JNK (1:1,000), p-JNK (1:800), c-Src (1:1,000) (all from Santa Cruz Biotechnology), p-Src (1:800), NF-κB (1:1,000), Nrf-2 (1:1,000), β-actin (1:1,000), or lamin B (1:1,000) (all from Enzo Life Sciences). The blots were washed three times and incubated with horseradish peroxidase-conjugated anti-rabbit immunoglobulin G (1:5,000) for 2 hours (Bethyl Laboratories, Montgomery, TX, USA). Blotting analysis was performed using the luminal Western blotting detection kit (Santa Cruz Biotechnology Inc) and a luminescent image analyzer (LAS-4000, Fujifilm, Tokyo, Japan).

Enzyme-linked immunosorbent assay

A549 cells were exposed to nanoparticles for designated times, and the supernatants were then collected, centrifuged to remove any remaining nanoparticles, and stored at –80°C. Concentrations of the proinflammatory cytokines, IL-1, IL-6, IL-8, and TNF-α, were determined by enzyme-linked immunosorbent assay, according to the instructions supplied by the manufacturer (BD Bioscience, Franklin Lakes, NJ, USA). Cells incubated without nanoparticles were used as controls. Absorbance was measured at 450 nm and quantified using a microplate reader (Dynex Technologies).

Inhibitors or antioxidant treatment

Cells were pretreated with a JNK inhibitor (SP600125, 10 μ M), a p38 inhibitor (SB203580, 5 μ M), or an SFK inhibitor (PP2, 5 μ M) for 1 hour, and then incubated with the nanoparticles. Expression levels of MAPK and SFK and induction of proinflammatory mediators were evaluated by Western blot analysis and enzyme-linked immunosorbent assay, respectively. Alternatively, A549 cells were preincubated with the antioxidant ascorbic acid (5 mM) for 2 hours, and then incubated with the nanoparticles. ROS generation, expression levels of MAPK or SFK, and induction of proinflammatory mediators were investigated as described above.

Statistical analysis

The statistical analysis was performed using the Student's *t*-test for unpaired data, and one-way analysis of variance (Tukey's test, version 11.0) was conducted using SAS software (SAS Institute, Cary, NC, USA) to determine the significance of differences between experimental groups. All results are presented as the mean \pm standard deviation and $P < 0.05$ were considered to be statistically significant.

Results

Characterization of LDH-NPs

The X-ray diffraction pattern for the LDH-NPs revealed a typical MgAl layered structure, as indicated by (003), (006), (009), and (110) peaks (Figure 1A). Fourier transform infrared data confirmed that MgAl-CO₃ LDH-NPs formed with peaks at 3,468.84, 1,633.91, 1,377.69, and 426.13 cm^{-1} , which were attributed to OH⁻ stretching, H₂O binding, CO₃⁻² group, and O-M-O vibration, respectively (Figure 1C). SEM images of LDH-NP showed a typical hexagonal shape and an average particle size of 102.55 \pm 13.62 nm (Figure 1B and D).

Cell proliferation and ROS generation

The cytotoxicity of LDH-NPs was evaluated by measuring cell proliferation/viability using the WST-1 assay. A549 cells were used because oxidative stress and IL-8 were highly induced in this cell line by LDH-NPs. Nanoparticles present at concentrations of up to 1,000 $\mu\text{g/mL}$ did not affect the proliferation or viability of cells after 24 hours of incubation (data not shown), and at a concentration of 500 $\mu\text{g/mL}$, LDH-NPs did not affect proliferation or viability when incubated for 1–24 hours (Figure 2A). However, LDH-NP generated ROS

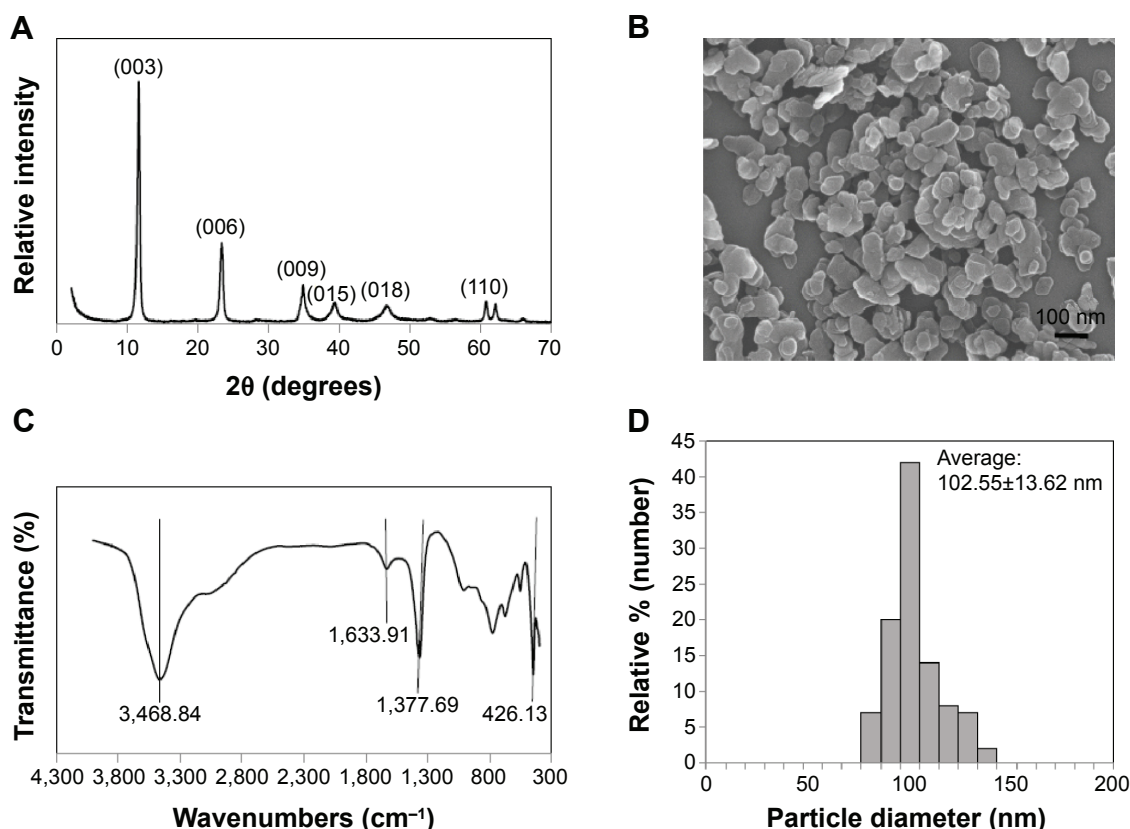


Figure 1 Physicochemical characterization of LDH-NPs. X-ray diffraction pattern (A), scanning electron micrographs (B), Fourier transform infrared data (C), and size distribution of LDH-NPs determined by randomly selecting 200 particles in scanning electron micrographs (D).
Abbreviation: LDH-NPs, layered double hydroxide nanoparticles.

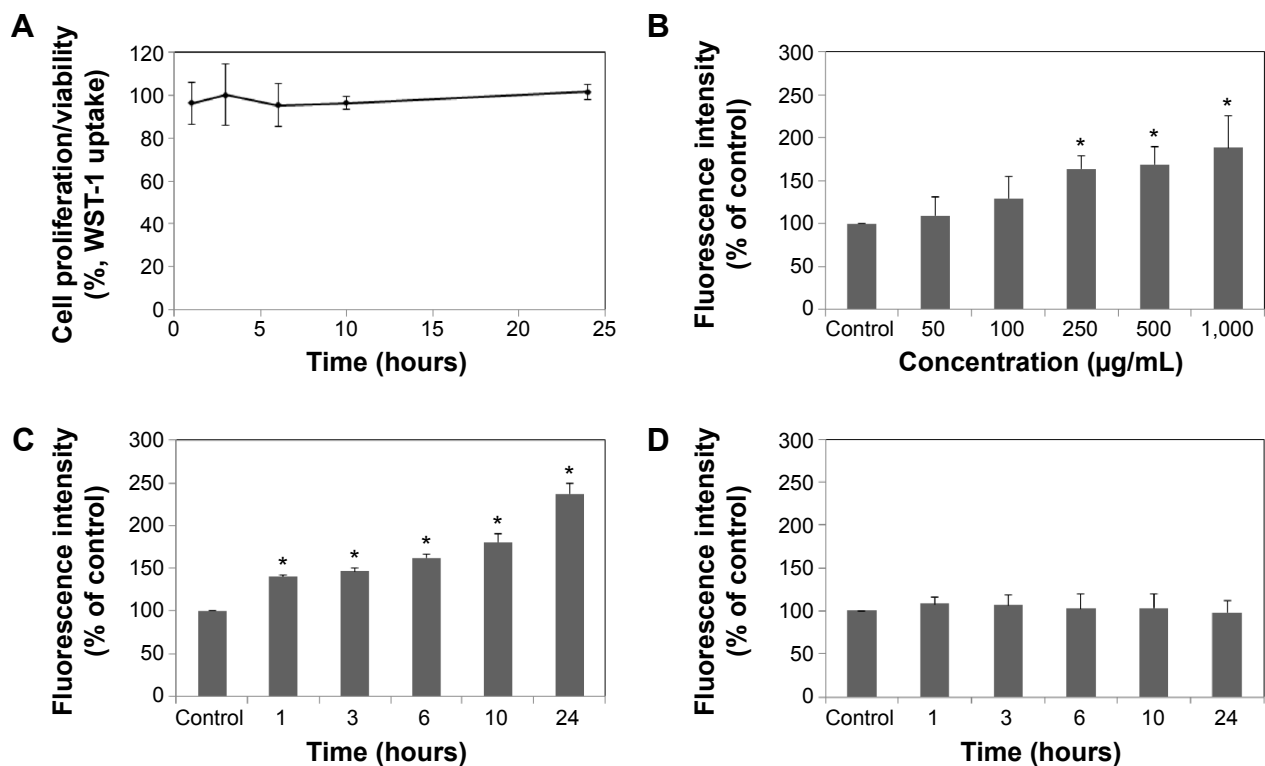


Figure 2 Cell proliferation of A549 cells treated with 500 μg/mL of LDH-NPs (A). Generation of reactive oxygen species by cells treated with different concentrations of LDH-NPs for 24 hours (B), 500 μg/mL LDH-NPs for different periods of time (C), and under the same conditions as those mentioned in (C) in the presence of an antioxidant, ascorbic acid (D).

Notes: The results are expressed as the mean ± standard deviation of three independent experiments. *Denotes a significant difference from the non-treated control ($P < 0.05$).

Abbreviation: LDH-NPs, layered double hydroxide nanoparticles.

in cells treated at 250–1,000 μg/mL for 24 hours (Figure 2B), and ROS levels were found to be elevated in cells exposed to 500 μg/mL LDH-NPs for 1–24 hours (Figure 2C). Interestingly, no significant increase in ROS levels was detected in LDH-NP-incubated cells in the presence of an antioxidant, ascorbic acid (Figure 2D). These results indicate that LDH-NPs generate ROS at high concentrations.

Antioxidant enzyme activity

The activity of several antioxidant enzymes was evaluated to examine changes in the levels of protective enzymes in A549 cells exposed to LDH-NPs. The activity of all the antioxidant enzymes examined, ie, that of CAT, GR, and SOD, were elevated by LDH-NPs at 250–1,000 μg/mL (Figure 3A, C, and E). Furthermore, enzyme activity was significantly increased by 500 μg/mL LDH-NPs after incubation for 1–24 hours (Figure 3B, D, and F), which agreed well with the observed generation of ROS by LDH-NPs (Figure 2B and C). In addition, HO-1 (an antioxidant enzyme induced in response to oxidative stress) activity was also significantly increased by LDH-NPs in a concentration-dependent and time-dependent manner (Figure 3G and H). These results

demonstrate that antioxidant enzyme activity, which plays a role in the scavenging of ROS, was increased by LDH-NPs, thus confirming induction of oxidative stress by LDH-NPs.

Cytokine induction

We also examined the effects of LDH-NPs on proinflammatory cytokines, ie, IL-1, IL-6, IL-8, and TNF-α. Levels of IL-1 and TNF-α were not significantly increased by LDH-NPs (data not shown), whereas IL-6 and IL-8 levels were considerably increased in a time-dependent manner (Figure 4A and B). On the other hand, elevation of IL-6 and IL-8 levels was significantly reduced in the presence of ascorbic acid, indicating the role of oxidative stress in cytokine induction.

Signal transduction and transcription factors

Molecular events were evaluated in A549 cells exposed to LDH-NPs in order to elucidate the mechanism responsible for their effects on oxidative stress and cytokine release. Expression of the phosphorylated forms of p38 and JNK was significantly elevated in cells exposed to LDH-NPs at

500–1,000 $\mu\text{g/mL}$ (Figure 5A). In particular, JNK phosphorylation was remarkably increased after incubation with 500 $\mu\text{g/mL}$ LDH-NP for only 1 hour (Figure 5B), whereas expression of ROS p-ERK did not change significantly (Figure 5). On the other hand, when the expression level of Src, which lies upstream of the MAPK pathway, was examined, its phosphorylation was found to be significantly increased after treatment with 500 $\mu\text{g/mL}$ LDH-NPs for 1–24 hours (Figure 6).

The molecular mechanism responsible for the toxicity of LDH-NPs was investigated further by examining the transcription factors, NF- κB and Nrf-2, which lie downstream of

the MAPK signaling pathway (Figure 7). Nuclear translocation of NF- κB was found to be promoted in a concentration-dependent manner (Figure 7A and C), whereas nuclear translocation of Nrf-2 was not (Figure 7B and D).

Relationship between SFK-MAPK signaling pathway and cytokine induction

Induction of IL-6 and IL-8 in cells treated with LDH-NPs was evaluated in the presence of an SFK inhibitor (PP2), a p38 inhibitor (SB203580), and a JNK inhibitor (SP600125). As shown in Figure 8, induction of IL-6 and IL-8 by LDH-NPs was considerably reduced by all three inhibitors.

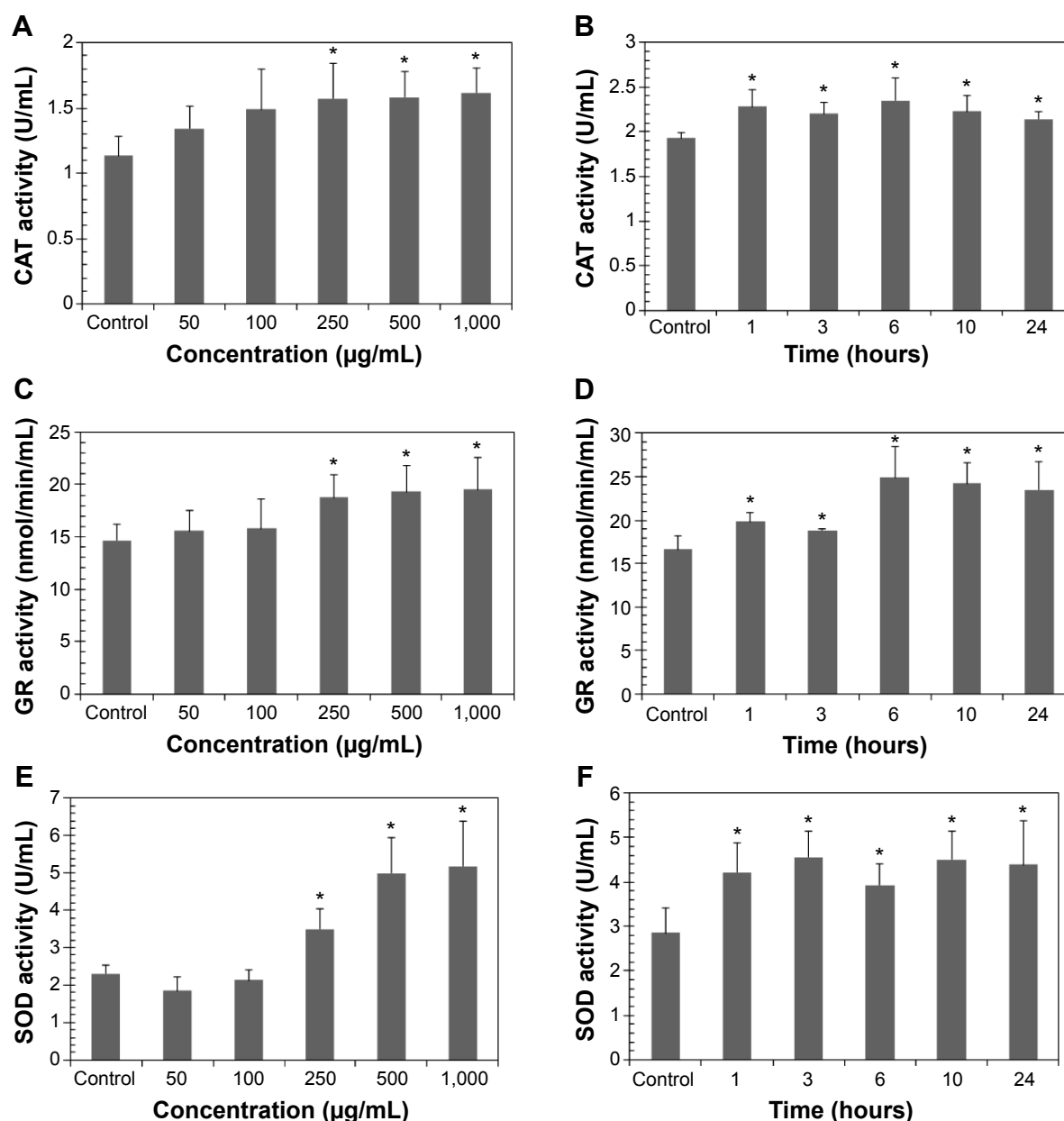


Figure 3 (Continued)

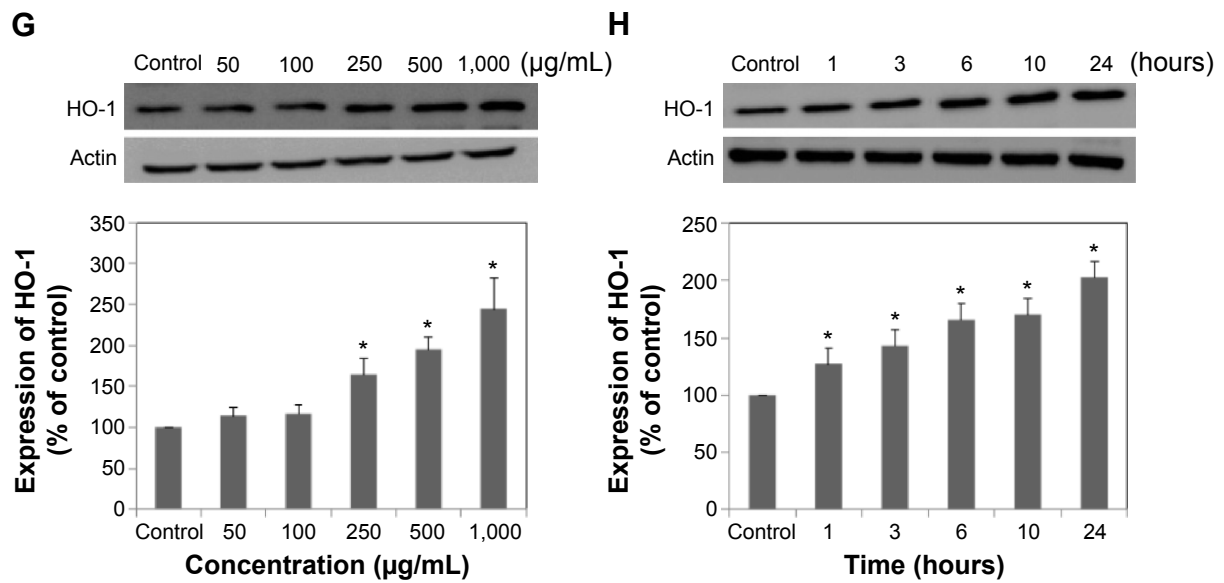


Figure 3 Activity of antioxidant enzymes in A549 cells exposed to LDH-NPs. For the concentration-dependent experiment, cells were incubated with LDH-NPs for 24 hours (A, C, E, G), and for the time-dependent experiment, cells were exposed to 500 µg/mL LDH-NPs (B, D, F, H).

Notes: The results are presented as the mean standard deviation of three independent experiments. *Denotes a significant difference from the non-treated control ($P < 0.05$).

Abbreviations: LDH-NPs, layered double hydroxide nanoparticles; CAT, catalase; GR, glucose reductase; SOD, superoxide dismutase; HO-1, heme oxygenase-1.

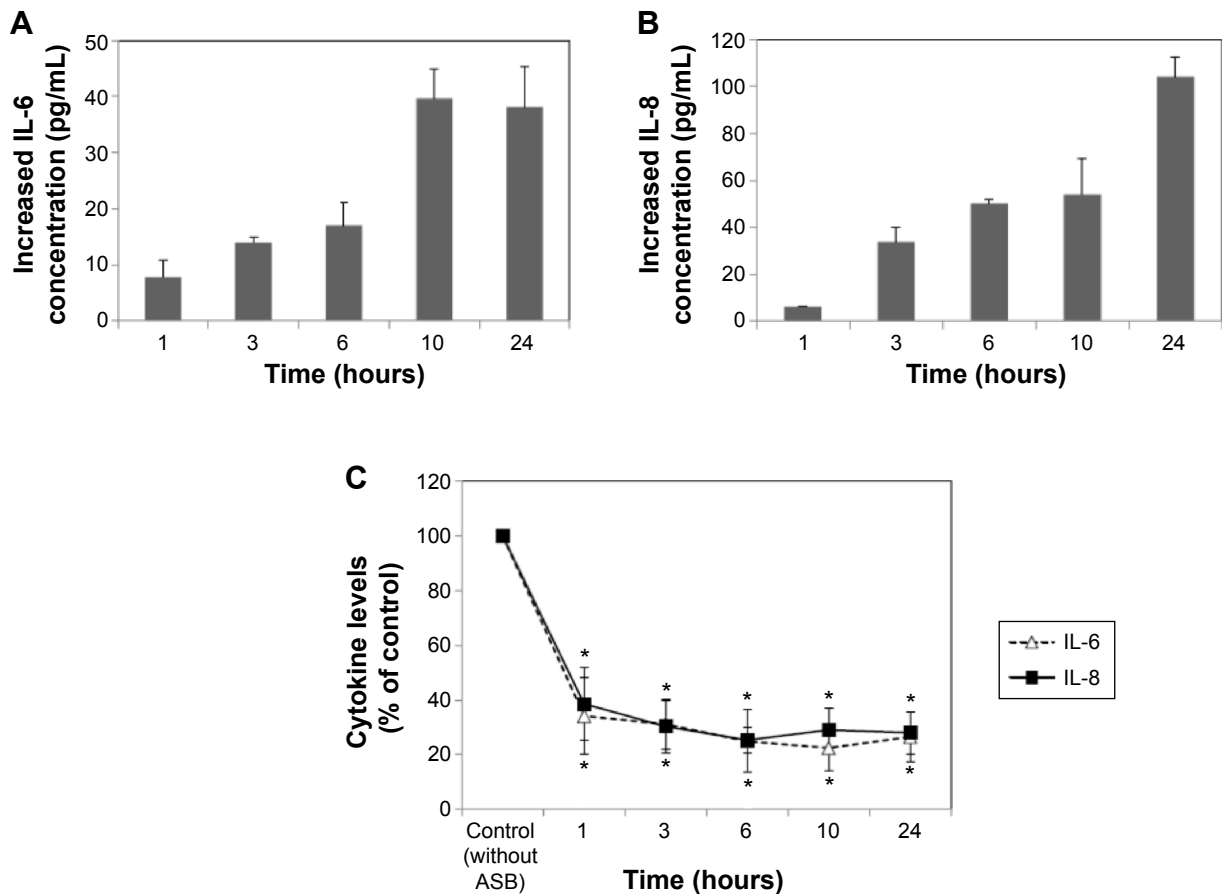


Figure 4 Induction of the proinflammatory cytokines IL-6 and IL-8 in A549 cells exposed to 500 µg/mL LDH-NPs (A, B) and under the same conditions in the presence of ASB (C). Cytokine concentrations are presented as increases in IL-6 or IL-8 levels after subtracting basal IL-6 or IL-8 levels detected in untreated controls.

Notes: The results are presented as the mean \pm standard deviation of three independent experiments. *Denotes a significant difference from the non-treated control ($P < 0.05$).

Abbreviations: ASB, ascorbic acid; IL, interleukin; LDH-NPs, layered double hydroxide nanoparticles.

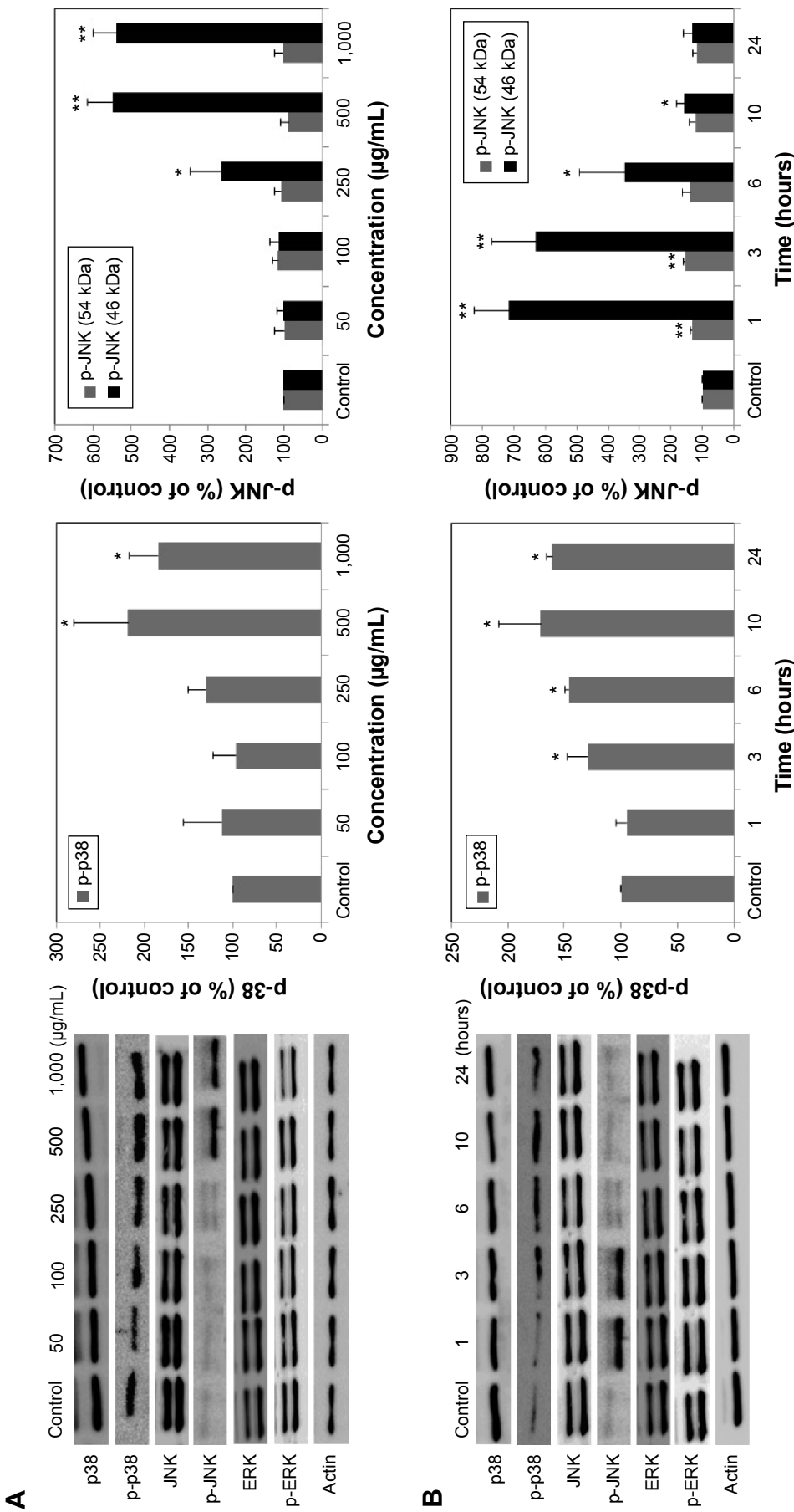


Figure 5 Expression of MAPK in A549 cells exposed to different concentrations of LDH-NPs for 24 hours (A) or to 500 µg/mL LDH-NPs for different time periods (B). Relative density of expression of ERK, JNK, and p-38 were normalized versus β-actin and are presented relative to the non-treated control.

Notes: The results are presented as the mean ± standard deviation of three independent experiments. *Denotes a significant difference from the non-treated control ($p < 0.05$), **Denotes a significant difference from the non-treated control ($p < 0.01$).

Abbreviations: LDH-NPs, layered double hydroxide nanoparticles; MAPK, mitogen-activated protein kinase; ERK, extracellular signal-regulated kinase; JNK, c-Jun-N-terminal kinase.

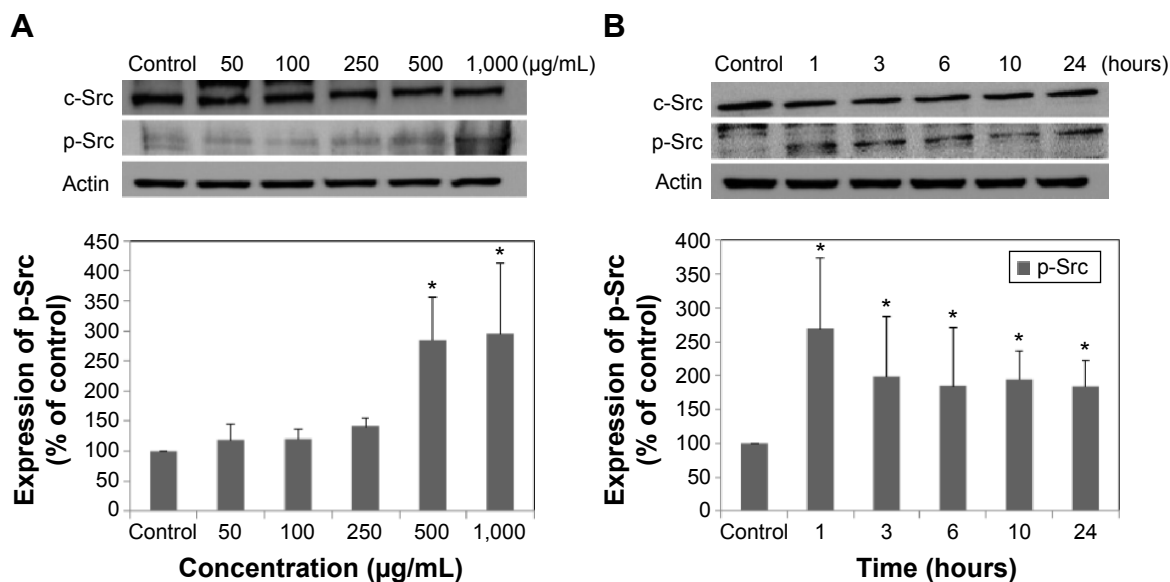


Figure 6 Expression of Src family kinases in A549 cells exposed to different concentrations of LDH-NPs for 24 hours (A) or to 500 µg/mL LDH-NPs for different time periods (B). The relative density of expression of c-Src (intact) and p-Src (phosphorylated) was normalized versus β -actin and is presented as relative to the non-treated control.

Notes: The results are presented as the mean \pm standard deviation of three independent experiments. *Denotes a significant difference from the non-treated control ($P < 0.05$).

Abbreviation: LDH-NPs, layered double hydroxide nanoparticles.

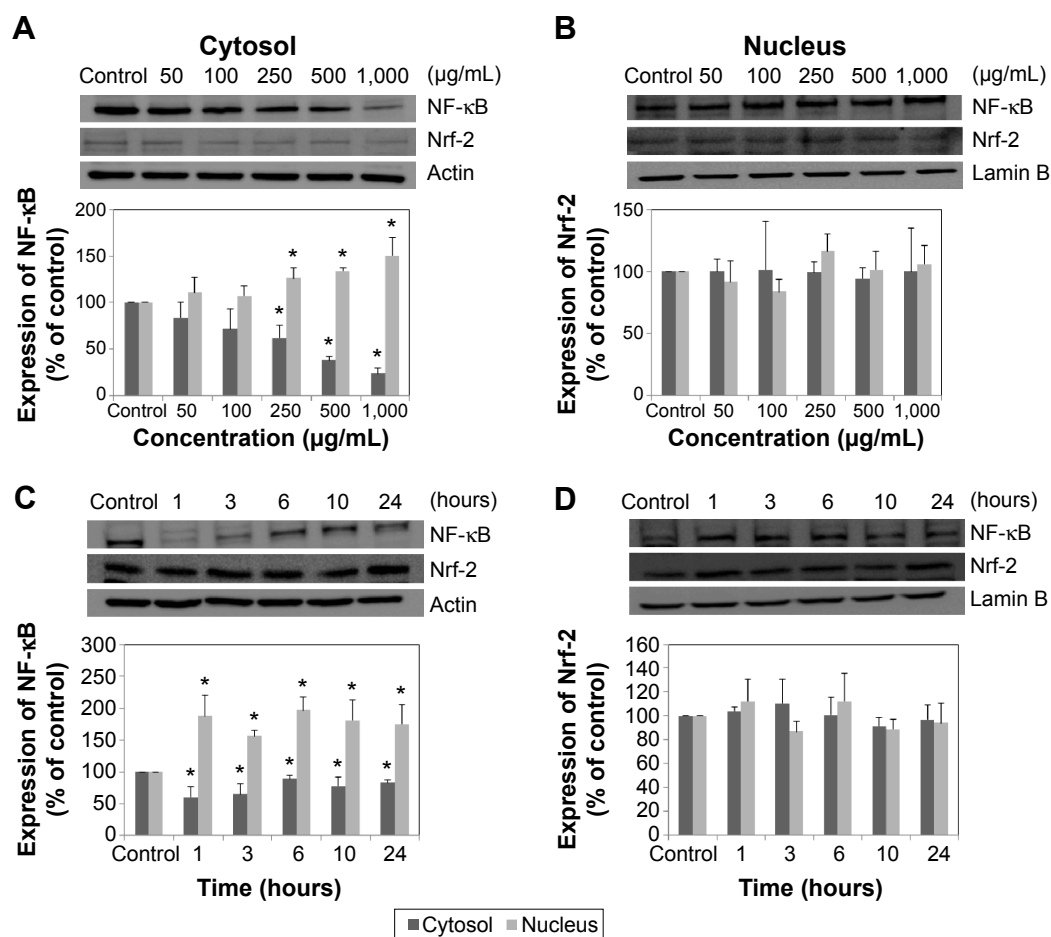


Figure 7 Expressions of NF- κ B and Nrf-2 in cytosolic and nuclear fractions of A549 cells exposed to different concentrations of LDH-NPs for 24 hours (A, B) or to 500 µg/mL LDH-NPs for different time periods (C, D). Relative density of expression of NF- κ B and Nrf-2 was normalized versus β -actin in cytosolic fractions or versus lamin B in nuclear fractions, respectively, and are presented relative to the non-treated control.

Notes: The results are presented as the mean \pm standard deviation of three independent experiments. *Denotes a significant difference from the non-treated control ($P < 0.05$).

Abbreviations: LDH-NPs, layered double hydroxide nanoparticles; NF- κ B, nuclear factor kappa B; Nrf-2, nuclear factor-erythroid 2-related factor-2.

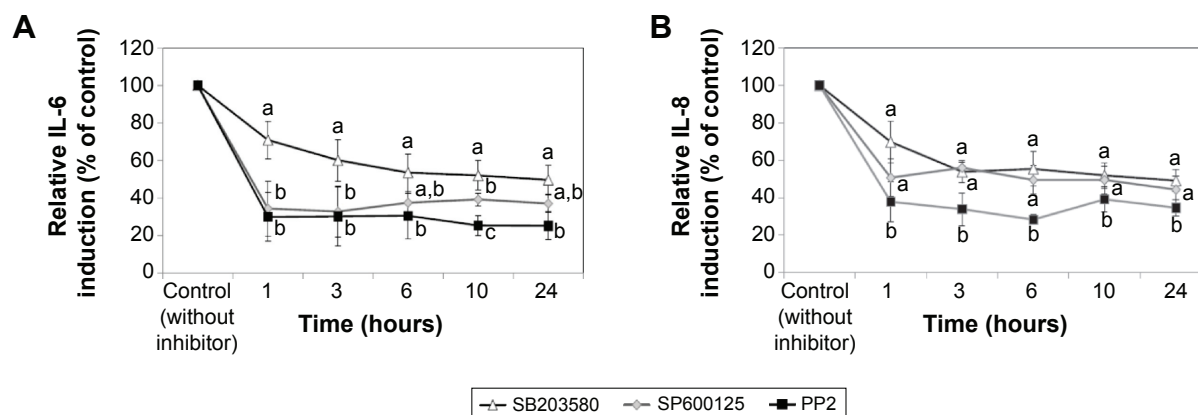


Figure 8 Involvement of SFKs, JNK, and p38 MAPK in LDH-NP-induced IL-6 (A) and IL-8 (B) release from A549 cells. Cells were exposed to 500 $\mu\text{g/mL}$ LDH-NPs only (controls) or pretreated with the p38 inhibitor SB203580, the JNK inhibitor SP600125, or the SFK inhibitor PP2, and then treated with 500 $\mu\text{g/mL}$ LDH-NPs for different time periods. Cytokine release was measured by enzyme-linked immunosorbent assay, according to the instructions supplied by the manufacturer (BD Bioscience).

Notes: The results represent the mean \pm standard deviation of three independent experiments and are presented as relative cytokine induction versus LDH-NP-treated controls (100% induction). Different letters in the figure indicate a statistically significant difference ($P < 0.05$).

Abbreviations: IL, interleukin; JNK, c-Jun-N-terminal kinase; SFKs, Src family kinases; LDH-NPs, layered double hydroxide nanoparticles; MAPK, mitogen-activated protein kinase.

In particular, both cytokine inductions were markedly diminished by PP2.

Discussion

This study was undertaken to evaluate the toxic effects of LDH-NP and to determine the molecular mechanism involved in relation to oxidative stress and inflammatory cytokine induction. Diverse types of nanoparticles have been reported to induce oxidative stress or inflammatory responses.^{28–30} However, few studies have addressed the mechanism responsible for nanoparticle-induced toxicity. In a previous study, we found that LDH-NPs generated ROS in human alveolar epithelial cancer A549 cells, human osteosarcoma (HOS) cells, and human cervical adenocarcinoma HeLa cells, but not in normal human lung epithelial L-132 cells, and because LDH-NP generated the most ROS and induced the proinflammatory mediator IL-8 in A549 cells, we used this cell line for the present study.¹¹ In terms of the effect of particle size on toxicity, LDH-NPs 50 nm in size were determined to be more toxic than 100–350 nm particles.³¹ However, small-sized particles less than 100 nm tend to form aggregates in cell culture medium, so 100 nm particles were selected for the mechanistic study.

The LDH-NPs used in the present study had a homogeneous distribution and a particle size of ~ 100 nm. A549 cells were exposed to high concentrations of LDH-NPs in the mechanistic study because ROS was found to be generated when cells were treated with LDH-NPs at 250–1,000 $\mu\text{g/mL}$ for 1–24 hours (Figure 2B) and because cytokine release was marked at more than 500 $\mu\text{g/mL}$ (data not shown). It is worthy of note that the actual concentration of LDH-NP as a delivery carrier is less than 100 $\mu\text{g/mL}$. Further, at 500 $\mu\text{g/mL}$,

LDH-NPs produced ROS within only 1 hour (Figure 2B), but notably, cell proliferation was unaffected by treatment with LDH-NPs at this concentration for 24 hours (Figure 2A). On the other hand, no significant increase in ROS levels was detected in cells exposed to LDH-NPs in the presence of ascorbic acid (Figure 2D), suggesting that ROS generation by LDH-NPs is associated with oxidative stress.

Oxidative stress induction by LDH-NPs was confirmed by analyzing the activity and induction of antioxidant enzymes. As shown in Figure 3, the activity of CAT (decomposes hydrogen peroxide to water and oxygen), GR (reduces glutathione disulfide to glutathione), and SOD (catalyzes the dismutation of superoxide radicals to oxygen and hydrogen peroxide) significantly increased in cells exposed to ≥ 250 $\mu\text{g/mL}$ LDH-NPs, and their enzyme activity increased after exposure for only 1 hour when A549 cells were treated with 500 $\mu\text{g/mL}$ LDH-NPs. On the other hand, HO-1 protein levels also increased in response to LDH-NP treatment (Figure 3G and H). Further, a strong correlation was observed between ROS generation (Figure 2B and C) and increased activity of the antioxidant enzymes (Figure 3). These results show that antioxidant activity increased in cells exposed to LDH-NP, probably to control and neutralize the ROS generated. These results may also explain why LDH-NPs did not affect cell proliferation (Figure 2A).

Western blot analysis revealed that phosphorylation of p38 was significantly induced in A549 cells exposed to LDH-NPs at concentrations ≥ 500 $\mu\text{g/mL}$ for 3–24 hours (Figure 5), whereas induction of phosphorylated JNK was observed after 1–10 hours at LDH-NP concentrations ≥ 250 $\mu\text{g/mL}$, that is, JNK was more strongly

and rapidly activated than p38. This suggests that JNK was activated immediately after exposure to LDH-NPs, and that activation of p38 was associated with regulation of LDH-NP-induced oxidative stress at a later stage. ERK expression remained constant after incubation with LDH-NPs. On the other hand, Src, which lies upstream of MAPK, was also activated in cells treated with LDH-NPs at high concentrations ($\geq 500 \mu\text{g/mL}$) at 1–24 hours (Figure 6), in a manner similar to that observed for JNK (Figure 5). Further, nuclear translocation of NF- κ B, which occurs downstream of MAPK, was increased at LDH-NP concentrations $\geq 250 \mu\text{g/mL}$ after 1–24 hours of exposure, whereas cytosolic and nuclear levels of Nrf-2 remained constant. These results suggest that LDH-NPs provoke oxidative stress, and that this subsequently induces activation of SFK, followed by activation of JNK and p38 MAPK, finally leading to activation of NF- κ B (Figure 9). Nuclear translocation of NF- κ B is likely to be primarily controlled by JNK after 1–6 hours, and p38 mediates NF- κ B translocation after prolonged exposure. Activation of NF- κ B signaling by LDH-NP has been demonstrated by Li et al but seems to be involved in activation of dendritic cells.³²

CeO₂ nanoparticles have been reported to cause oxidative stress and subsequent induction of HO-1 via a p38-Nrf-2 signaling pathway.²⁶ However, oxidative stress and

expression of molecular entities associated with oxidative stress-related events were induced after 24 hours of exposure to a low concentration (1 $\mu\text{g/mL}$) of CeO₂ nanoparticles.²⁶ This contrasts with what was observed for LDH-NPs because they generated ROS and activated signaling pathways at concentrations exceeding 250 $\mu\text{g/mL}$ after incubation for 1–24 hours. Further, it has been reported that oxidative stress caused by both fumed and porous silica nanoparticles (1 $\mu\text{g/mL}$) activated Nrf-2 via the ERK MAPK signaling pathway after incubation for 24 hours.³³ In another study, single-walled carbon nanotubes (10 $\mu\text{g/mL}$) were found to induce oxidative stress and augment activation of NF- κ B in human keratinocytes, but unfortunately the upstream signaling mechanism involved was not investigated.³⁴

The toxic effects of LDH-NPs have also been reported to be due to induction of the proinflammatory mediator, IL-8.^{11,31} In the present study, LDH-NPs were found to induce IL-6 and IL-8 (Figure 4A and B), but not IL-1 or TNF- α in A549 cells (data not shown). Interestingly, induction of IL-6 and IL-8 by LDH-NPs was highly suppressed in the presence of ascorbic acid (Figure 4C), suggesting that oxidative stress caused by LDH-NPs plays an important role in induction of cytokines. It is worth noting that induction of IL-6 and IL-8 by LDH-NPs was highly suppressed by pretreating cells with SFK, JNK, or p38 inhibitors (Figure 8). Further,

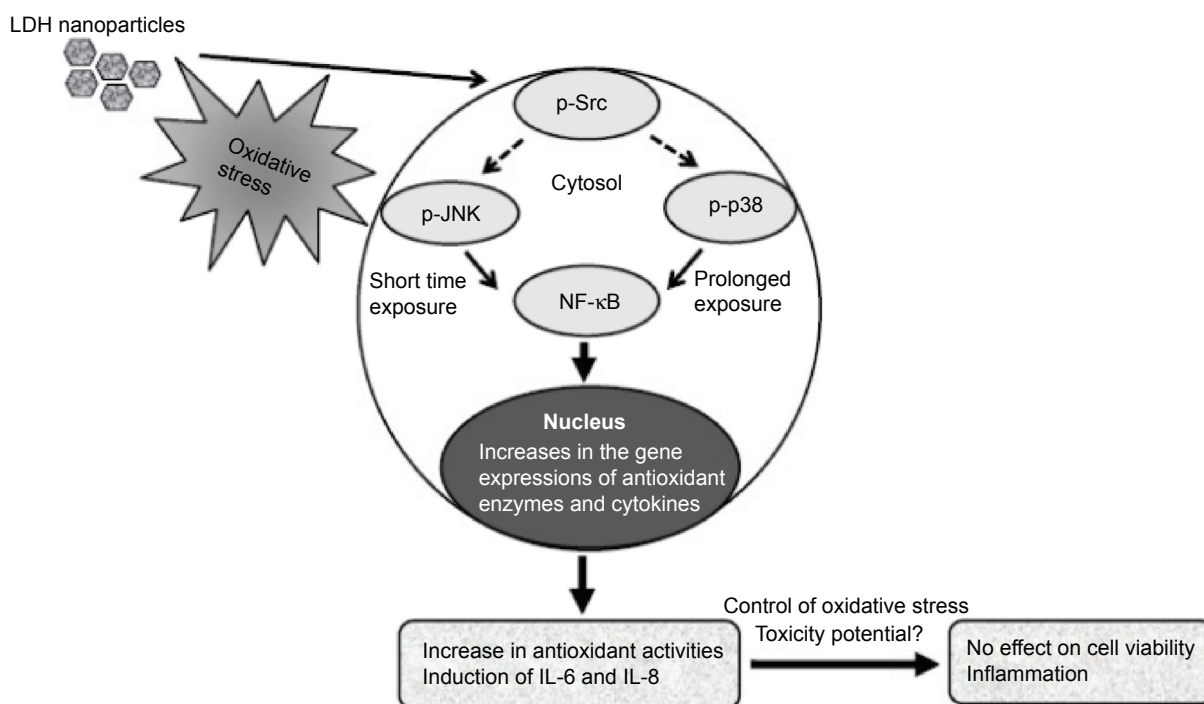


Figure 9 Schematic illustration of the proposed mechanism of LDH-NP-induced toxicity in A549 cells. Oxidative stress caused by LDH-NPs activates SFK-JNK and p38-NF- κ B signaling pathway, which increases expression of protective antioxidant enzymes, such as CAT, GR, SOD, and HO-1. However, this signaling activation concomitantly leads to induction of the proinflammatory mediators, IL-6 and IL-8.

Abbreviations: IL, interleukin; JNK, c-Jun-N-terminal kinase; SFK, Src family kinase; LDH-NPs, layered double hydroxide nanoparticles; NF- κ B, nuclear factor kappa B; CAT, catalase; GR, glucose reductase; SOD, superoxide dismutase; HO-1, heme oxygenase-1.

inhibition of SFK, which acts upstream of the JNK and p38 signaling pathways, most effectively suppressed cytokine induction, indicating that cytokine release is governed by the SFK-JNK and SFK-p38 MAPK pathways. Based on the observation that IL-6 release was considerably reduced by pretreating cells with the JNK inhibitor SP600125, JNK activation appears to be closely related to IL-6 induction. A small number of studies have shown that nanoparticle-induced oxidative stress contributes to the inflammatory response. For example, it has been reported that single-wall carbon nanotubes induce ROS and activate the MAPK and NF- κ B signaling pathways, which are associated with the inflammatory response,¹⁴ and that multiwalled carbon nanotubes induce a fibrogenic response via ROS-mediated activation of NF- κ B signaling.³⁵ Titanium dioxide nanoparticles have been reported to induce oxidative stress and IL-8 release through the p38 and/or ERK MAPK pathways in BEAS-2B cells.³⁶ p38 and SFK-ERK1/2 pathways were found to regulate crystalline silica-induced IL-8 release in A549 cells, although ROS generation was not examined.²⁸ It was interesting that cell proliferation was unaffected by LDH-NPs in the present study, and that LDH-NPs, unlike other nanoparticles, induced oxidative stress at high concentrations. We believe that this is probably associated with the increased activity of antioxidant enzymes via the SFK-JNK and p38-NF- κ B signaling pathway. Coincidentally, activation of the SFK-JNK and p38-NF- κ B pathway via the oxidative stress induced by LDH-NPs led to induction of IL-6 and IL-8, suggesting that LDH-NPs have inflammatory potential (Figure 9).

Conclusion

Our results suggest that the toxic effects of LDH-NPs are due to oxidative stress, which can also provoke induction of proinflammatory cytokines. The study shows that exposure to LDH-NPs induces ROS and expression of antioxidant enzymes, such as CAT, GR, SOD, and HO-1, via a SFK-JNK and p38-NF- κ B signaling pathway, and that these protect against LDH-NP-induced oxidative stress. Further, activation of this signaling pathway concomitantly induces expression of proinflammatory cytokines, including IL-6 and IL-8. Therefore, it is likely that oxidative stress caused by LDH-NP mediates the inflammatory response in human lung epithelial cells.

Acknowledgments

This research was supported by the Basic Science Research Program through the National Research Foundation of Korea

(NRF) funded by the Ministry of Science, ICT, and Future Planning (2013R1A1A3009283), and by Nano Material Technology Development Program (2014M3A7B6020163) of MSIP/NRF.

Disclosure

The authors report no conflicts of interest in this work.

References

- Barry RC, Lin Y, Wang J, Liu G, Timchalk CA. Nanotechnology-based electrochemical sensors for biomonitoring chemical exposures. *J Expo Sci Environ Epidemiol*. 2009;19:1–18.
- Cormode DP, Skajaa T, Fayad ZA, Mulder WJ. Nanotechnology in medical imaging: probe design and applications. *Arterioscler Thromb Vasc Biol*. 2009;29:992–1000.
- Choi SJ, Lee JK, Jeong J, et al. Toxicity evaluation of inorganic nanoparticles: considerations and challenges. *Mol Cell Toxicol*. 2013; 9:205–210.
- Krpetic Z, Anguissola S, Garry D, Kelly PM, Dawson KA. Nanomaterials: impact on cells and cell organelles. *Adv Exp Med Biol*. 2014; 811:135–156.
- Shang L, Nienhaus K, Nienhaus GU. Engineered nanoparticles interacting with cells: size matters. *J Nanobiotechnology*. 2014;12:5.
- Choi SJ, Choy JH. Effect of physico-chemical parameters on the toxicity of inorganic nanoparticles. *J Mater Chem*. 2011;21:5547–5554.
- Choi SJ, Choy JH. Layered double hydroxide nanoparticles as target-specific delivery carriers: uptake mechanism and toxicity. *Nanomedicine (Lond)*. 2011;6:803–814.
- Evans DG, Duan X. Preparation of layered double hydroxides and their applications as additives in polymers, as precursors to magnetic materials and in biology and medicine. *Chem Commun (Camb)*. 2006;5:485–496.
- Choy JH, Choi SJ, Oh JM, et al. Clay minerals and layered double hydroxides for novel biological applications. *Appl Clay Sci*. 2007;36: 122–132.
- Kura AU, Hussein MZ, Fakurazi S, Arulselvan P. Layered double hydroxide nanocomposite for drug delivery systems; bio-distribution, toxicity, and drug activity enhancement. *Chem Cent J*. 2014;8:47.
- Choi SJ, Oh JM, Choy JH. Toxicological effects of inorganic nanoparticles on human lung cancer A549 cells. *J Inorg Biochem*. 2009; 103:463–471.
- Manke A, Wang L, Rojanasakul Y. Mechanism of nanoparticle-induced oxidative stress and toxicity. *Biomed Res Int*. 2013;2013:92916.
- Donaldson K, Poland CA. Inhaled nanoparticles and lung cancer – what we can learn from conventional particle toxicology. *Swiss Med Wkly*. 2012;142:w13547.
- Pacurari M, Yin XJ, Zhao J, et al. Raw single-wall carbon nanotubes induce oxidative stress and activate MAPKs, AP-1, NF- κ B, and Akt in normal and malignant human mesothelial cells. *Environ Health Perspect*. 2008;116:1211–1217.
- Takeda K, Matsuzawa A, Nishitoh H, et al. Roles of MAPKKK ASK1 in stress-induced cell death. *Cell Struct Funct*. 2003;28:23–29.
- Jayakumar AR, Panickar KS, Murthy ChR, Norenberg MD. Oxidative stress and mitogen-activated protein kinase phosphorylation mediate ammonia-induced cell swelling and glutamate uptake inhibition in cultured astrocytes. *J Neurosci*. 2006;26:4774–4484.
- Puddicombe SM, Davies DE. The role of MAP kinases in intracellular signal transduction in bronchial epithelium. *Clin Exp Allergy*. 2000; 30:7–11.
- Li DQ, Luo L, Chen Z, et al. JNK and ERK MAP kinases mediate induction of IL-1 β , TNF- α and IL-8 following hyperosmolar stress in human limbal epithelial cells. *Exp Eye Res*. 2006;82:588–596.

19. Hsu HY, Chiu SL, Wen MH, Chen KY, Hua KF. Ligands of macrophage scavenger receptor induce cytokine expression via differential modulation of protein kinase signaling pathways. *J Biol Chem*. 2001; 276:28719–28730.
20. Kitagawa D, Tanemura S, Ohata S, et al. Activation of extracellular signal-regulated kinase by ultraviolet is mediated through Src-dependent epidermal growth factor receptor phosphorylation. Its implication in an anti-apoptotic function. *J Biol Chem*. 2002;277:366–371.
21. Pinkus R, Weiner LM, Daniel V. Role of oxidants and antioxidants in the induction of AP-1, NF-kappaB, and glutathione S-transferase gene expression. *J Biol Chem*. 1996;271:13422–13429.
22. Jin W, Wang H, Yan W, et al. Disruption of Nrf2 enhances upregulation of nuclear factor-kappaB activity, proinflammatory cytokines, and intercellular adhesion molecule-1 in the brain after traumatic brain injury. *Mediat Inflamm*. 2008;2008:725174.
23. Owuor ED, Kong AN. Antioxidants and oxidants regulated signal transduction pathways. *Biochem Pharm*. 2002;64:765–770.
24. Itoh K, Chiba T, Takahashi S, et al. An Nrf2/small Maf heterodimer mediates the induction of phase II detoxifying enzyme genes through antioxidant response elements. *Biochem Biophys Res Commun*. 1997;236: 313–322.
25. Zhang X, Chen X, Song H, Chen HZ, Rovin BH. Activation of the Nrf2/antioxidant response pathway increases IL-8 expression. *Eur J Immunol*. 2005;35:3258–3267.
26. Eom HJ, Choi J. Oxidative stress of CeO₂ nanoparticles via p38-Nrf-2 signaling pathway in human bronchial epithelial cell, Beas-2B. *Toxicol Lett*. 2009;187:77–83.
27. Wang J, Li N, Zheng L, et al. P38-Nrf-2 signaling pathway of oxidative stress in mice caused by nanoparticulate TiO₂. *Biol Trace Elem Res*. 2011;140:186–197.
28. Ovreivik J, Lag M, Schwarze P, Refsnes M. p38 and Src-ERK1/2 pathways regulate crystalline silica-induced chemokine release in pulmonary epithelial cells. *Toxicol Sci*. 2004;81:480–490.
29. Park EJ, Park K. Oxidative stress and pro-inflammatory responses induced by silica nanoparticles in vivo and in vitro. *Toxicol Lett*. 2009; 184:18–25.
30. Foucaud L, Goulaouic S, Bennisroune A, et al. Oxidative stress induction by nanoparticles in THP-1 cells with 4-HNE production: stress biomarker or oxidative stress signalling molecule? *Toxicol In Vitro*. 2010;24:1512–1520.
31. Choi SJ, Oh JM, Choy JH. Safety aspect of inorganic layered nanoparticles: size-dependency in vitro and in vivo. *J Nanosci Nanotechnol*. 2008; 8:5297–5301.
32. Li A, Qin L, Zhu D, Zhu R, Sun J, Wang S. Signalling pathways involved in the activation of dendritic cells by layered double hydroxide nanoparticles. *Biomaterials*. 2010;31:748–756.
33. Eom HJ, Choi J. Oxidative stress of silica nanoparticles in human bronchial epithelial cell, Beas-2B. *Toxicol In Vitro*. 2009;23:1326–1332.
34. Manna SK, Sarkar S, Barr J, et al. Single-walled carbon nanotube induces oxidative stress and activates nuclear transcription factor-kappaB in human keratinocytes. *Nano Lett*. 2005;5:1676–1684.
35. He X, Young SH, Schwegler-Berry D, Chisholm WP, Fernback JE, Ma Q. Multiwalled carbon nanotubes induce a fibrogenic response by stimulating reactive oxygen species production, activating NF-kappaB signaling, and promoting fibroblast-to-myofibroblast transformation. *Chem Res Toxicol*. 2011;24:2237–2248.
36. Park EJ, Yi J, Chung KH, Ryu DY, Choi J, Park K. Oxidative stress and apoptosis induced by titanium dioxide nanoparticles in cultured BEAS-2B cells. *Toxicol Lett*. 2008;180:222–229.

International Journal of Nanomedicine

Publish your work in this journal

The International Journal of Nanomedicine is an international, peer-reviewed journal focusing on the application of nanotechnology in diagnostics, therapeutics, and drug delivery systems throughout the biomedical field. This journal is indexed on PubMed Central, MedLine, CAS, SciSearch®, Current Contents®/Clinical Medicine,

Submit your manuscript here: <http://www.dovepress.com/international-journal-of-nanomedicine-journal>

Dovepress

Journal Citation Reports/Science Edition, EMBase, Scopus and the Elsevier Bibliographic databases. The manuscript management system is completely online and includes a very quick and fair peer-review system, which is all easy to use. Visit <http://www.dovepress.com/testimonials.php> to read real quotes from published authors.